

This is the author's copy of the publication as archived with the DLR's electronic library at <http://elib.dlr.de>. Please consult the original publication for citation.

Virtual Inertia as an Energy Dissipation Element for Haptic Interfaces

Hyeonseok Choi, Nam Gyun Kim, Aghil Jafari, Harsimran Singh, and Jee-Hwan Ryu

Copyright Notice





© 2022 IEEE. Personal use of this material is permitted. Permission from IEEE must be obtained for all other uses, in any current or future media, including reprinting/republishing this material for advertising or promotional purposes, creating new collective works, for resale or redistribution to servers or lists, or reuse of any copyrighted component of this work in other works.

Citation Notice

```
@ARTICLE{9689941,  
  author={Choi, Hyeonseok and Kim, Nam Gyun and Jafari, Aghil and Singh, Harsimran and Ryu, Jee-Hwan},  
  journal={IEEE Robotics and Automation Letters},  
  title={Virtual Inertia as an Energy Dissipation Element for Haptic Interfaces},  
  year={2022},  
  volume={7},  
  number={2},  
  pages={2708-2715},  
  doi={10.1109/LRA.2022.3144492}}
```

[1] H. Choi, N. G. Kim, A. Jafari, H. Singh and J. -H. Ryu, "Virtual Inertia as an Energy Dissipation Element for Haptic Interfaces," in *IEEE Robotics and Automation Letters*, vol. 7, no. 2, pp. 2708-2715, April 2022, doi: 10.1109/LRA.2022.3144492.

Virtual Inertia as an Energy Dissipation Element for Haptic Interfaces

Hyeonseok Choi , Nam Gyun Kim , Aghil Jafari , Harsimran Singh ,
and Jee-Hwan Ryu , *Senior Member, IEEE*

Abstract—Adding virtual damping to dissipate energy has been a major tool for designing stable haptic interfaces in most passivity-based approaches. However, virtual damping is known to dissipate a limited amount of energy. It even generates energy during high-velocity interaction because of the digitization effect, such as zero-order hold and quantization. Therefore, no proper energy dissipation element has been available to stabilize the interaction when the virtual damping is no longer functioning. This paper investigates the possibility of using virtual inertia as a complementary energy dissipation element of virtual damping for stable haptic interfaces. This paper analyzes the energy behavior of virtual inertia in the digital domain and finds that it can dissipate energy even in higher velocity interactions, unlike digital damping and digital springs. Furthermore, this paper proposes a unidirectional virtual inertia that can dissipate a considerable amount of energy compared with the conventional virtual inertia by storing energy and disappearing without returning it to the system. Simulation and experimental studies using a PHANTOM haptic interface proved the performance of the proposed method.

Index Terms—Force Control, haptics and haptic interfaces, physical human-robot interaction.

I. INTRODUCTION

STABLE interaction with high-stiffness virtual environments (VEs) is challenging, typically for impedance-type haptic interfaces. Studies have demonstrated that the maximum achievable impedance with a digital control loop is limited by time discretization [1], position quantization owing to encoder-based

position sensing [2], and the zero-order hold (ZOH) of the force signal by each servo cycle [3]. These effects cause the system to leak (that means generate) energy; if this energy cannot be dissipated via the intrinsic damping of a haptic device, the action of the controller, or damping by a human operator, the haptic interaction becomes unstable.

As part of the effort to achieve stable haptic interaction with high-stiffness virtual or remote environments, a significant amount of research has been conducted. One of the earlier studies used virtual coupling [4], but the achievable impedance of this approach is limited by the virtual spring and damper's impedance. Several methods have been proposed to increase the stability range by adding a constant [5], adaptive virtual damping [6], [7], and feed-forward force [8]. However, studies have shown, both numerically and experimentally, that only a limited range of virtual damping can be added to a system [9], [10] because virtual damping, unlike actual damping, is a discrete element and may itself even generate energy during a high stiffness and velocity interaction because of the digitization effect, such as ZOH and quantization. Moreover, rather than enlarging the impedance range, these methods shift it.

Recently, researchers have begun to focus on virtual inertia. Studies on virtual inertia rendering have been widely conducted. Colonnese and Okamura [11] analyzed the dynamic range of virtual inertia renderable in a stable manner. However, the studies were based on continuous systems, although haptic devices interact with discrete and VEs. Gil *et al.* [12] studied the stability conditions of a virtual spring–mass–damper in a digital interface. By analyzing the roots of the characteristic polynomial of a discrete-time state-space system, Desai *et al.* [13] demonstrated that the virtual mass feedback, up to the mass of the device, can enlarge the stiffness range. However, these two studies were limited to simply modeled linear systems. Moreover, studies on inertia compensation were conducted. Inertia compensation can be interpreted as rendering a negative virtual mass; however, its behavior is different from that of a normal positive virtual mass [14]. Studies on inertia compensation have mostly been conducted for medical robotics, such as dynamic compensation for a surgical teleoperation system [15] and inertia compensation for a lower-leg exoskeleton [16]. Gil *et al.* [17] explored inertia compensation using force feedforward for an impedance haptic device using additional sensors to estimate acceleration. In [18], the authors attempted to reduce the apparent inertial effect of haptic devices and overcome dynamic coupling because a user must experience the inertia of the manipulated object rather than

Manuscript received September 8, 2021; accepted January 6, 2022. Date of publication January 21, 2022; date of current version February 1, 2022. This work was supported in part by the National Research Foundation of Korea under Grant NRF-2020R1A2C200416912 and in part by the Ministry of Trade, Industry and Energy of Korea under Grant 20008957. This letter was recommended for publication by Associate Editor M. Frego and Editor A. Peer upon evaluation of the reviewers' comments. (Hyeonseok Choi and Nam Gyun Kim are co-first authors.) (Corresponding author: Jee-Hwan Ryu.)

Hyeonseok Choi is with the School of Mechanical Engineering, Korea University of Technology and Education, Cheonan 13557, Korea (e-mail: nam96bird@kaist.ac.kr).

Nam Gyun Kim is with the Robotics Program, KAIST 34141, Daejeon, Korea (e-mail: nam96bird@kaist.ac.kr).

Aghil Jafari is with the University of the West of England, Bristol BS16 1QY, U.K. (e-mail: aghiljafari1985@gmail.com).

Harsimran Singh is with the Institute of Robotics, and Mechatronics, German Aerospace Center, Wessling 82234, Germany (e-mail: harsimran.singh@dlr.de).

Jee-Hwan Ryu is with the Department of Civil and Environmental Engineering, Korea Advanced Institute of Science and Technology (KAIST), Daejeon 34141, Korea (e-mail: jhryu@kaist.ac.kr).

This letter has supplementary downloadable material available at <https://doi.org/10.1109/LRA.2022.3144492>, provided by the authors.

Digital Object Identifier 10.1109/LRA.2022.3144492

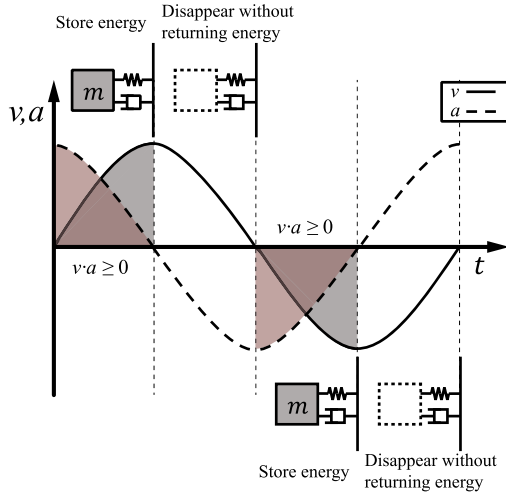


Fig. 1. Schematic of the concept of unidirectional virtual inertia, where v is the velocity, and a is the acceleration.

the inertia of the haptic device. *However, none of these studies considered virtual inertia as an energy dissipation element.*

For the first time, this paper investigates the possibility of using virtual inertia as an energy dissipation element, similar to virtual damping. This paper analyzes the energy dissipation ability of virtual inertia based on its energy behavior. The presented analyses are not limited to linear systems. These include the discrete interface of the VEs.

The main contributions of this paper are as follows: 1) to unveil the possibility of using virtual inertia as an energy dissipation element even in higher velocity interactions, unlike digital damping and a digital spring; 2) to propose a novel unidirectional virtual inertia that can dissipate a considerable amount of energy compared with the conventional virtual inertia and damping by causing the inertia to disappear after absorbing energy, without returning it to the system, as conceptually illustrated in Fig. 1. Simulation and experimental evaluations using a PHANTOM haptic interface validated the performance of the proposed method.

The remainder of this paper is organized as follows: Section II graphically interprets the energy leak of a haptic interface caused by time discretization, position quantization, and ZOH. Section III analyzes the energy behavior of virtual inertia. Section IV proposes the unidirectional virtual inertia as an energy dissipation element. Section V validates the proposed method with simulations and experiments. Section VI concludes the paper and provides discussions.

II. ENERGY LEAK IN HAPTIC INTERFACES

Fig. 2 shows the classical view of an impedance-type haptic interface with an open-loop impedance control where a human operator interacts with a VE through a haptic device that is a discrete model and simulated using a computer. The continuous and discrete domains are traditionally interconnected via a discrete interface by transmitting the sensed haptic device velocity (v) and commanding the force (f) back from the VE to the ZOH. This interconnection is known to generate energy and

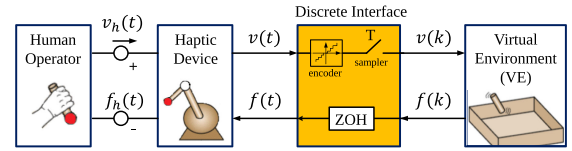


Fig. 2. Classical implementation of a haptic simulation composed of a human operator, haptic device, discrete interface, and virtual environment.

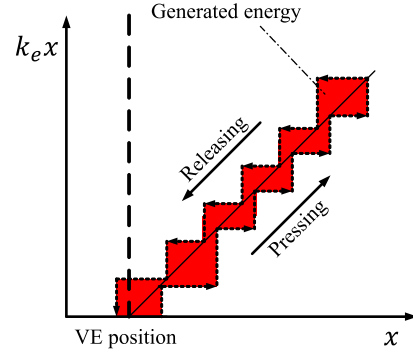


Fig. 3. Position versus force trajectory in a single contact. Signals are captured in between the haptic device and discrete interface.

cause unstable behavior, even in a simple spring-like VE:

$$f(k) = k_e x(k) \quad \forall k \geq 0 \quad (1)$$

where k_e is the stiffness constant of the VE.

The discrete interface is known to be a major source of energy leaks and instability. To demonstrate the energy leak based on the mathematical definition of passivity, velocity (v) versus force (f) can be used as follows:

$$\int_0^t f(\tau) v(\tau) d\tau \geq 0 \quad \forall t \geq 0 \quad (2)$$

where for simulated forces (f) and haptic device velocities (v), the integral of their product over time must be positive if the system dissipates energy [19], [20].

Fig. 3 shows the position versus force behavior when the human operator makes a single contact with a spring-like VE with stiffness k_e . The solid line shows the behavior of an ideal VE (a physical spring), whereas the dashed line shows the actual behavior of the discrete VE. The position versus force graph shows a staircase-shaped behavior because of discretization effects, such as discrete-time sampling, a limited resolution of the position sensor, and the ZOH effect. The area below the pressing trajectory is the input energy into the VE, and the area below the releasing trajectory is the output energy from the VE. Owing to quantization effects, the output force increases after the operator establishes contact with the VE. The output force decreases after the operator intends to release the haptic probe, and it ends after the operator is no longer in contact with the VE. This causes the output energy to be greater than the input energy, which indicates that the system is not passive and generates energy in each haptic interaction, which is the cause of instability.

In the discrete domain, the left-hand term in (2) can be interpreted as follows:

$$\sum_{k=0}^n f(k-1)v(k)\Delta T \quad (3)$$

or

$$\sum_{k=0}^n f(k-1)(x(k) - x(k-1)) \quad (4)$$

and with (1)

$$\sum_{k=0}^n k_e x(k-1)(x(k) - x(k-1)) \quad (5)$$

In the above equations, a one-step delay ($k-1$) is considered for the VE force (f) to calculate the energy [21]. This is because the output force increases after the operator establishes contact with the VE owing to quantization. It decreases after the operator intends to release the haptic probe. As (4) and Fig. 3 indicate that the vertical axis (f) is affected by the delay ($k-1$), the graph tends to shift toward the positive side of the horizontal axis (x) for the pressing path and toward the negative side of the horizontal axis (x) for the releasing path. All these shifts form a counterclockwise hysteresis-like behavior (Fig. 3), which means that the area under the releasing path is greater than the pressing path. This results in the generation of energy (red area highlighted in Fig. 3), and the interaction is not passive.

III. ENERGY BEHAVIOR OF VIRTUAL INERTIA

In this section, we analyze the energy behavior while rendering a virtual inertia (m). The simulated haptic force in the discrete domain can be calculated by multiplying m by the acceleration of the haptic device (a):

$$f(k) = ma(k) \quad \forall k \geq 0 \quad (6)$$

To calculate the pure energy contribution from the virtual inertia (whether generated or dissipated), we use (3) to include quantization and ZOH effects as in virtual damping and springs. Therefore, we obtained the net energy input ($E(n)$) from the virtual inertia:

$$\begin{aligned} E(n) &= \sum_{k=0}^n f(k-1)v(k)\Delta T \\ &= \sum_{k=0}^n ma(k-1)v(k)\Delta T, \end{aligned} \quad (7)$$

where v is the velocity of the haptic device, which is either numerically estimated from the encoder or directly measured from the accelerometer. The above equation can be simplified as follows:

$$E(n) = \sum_{k=0}^n E_{step}(k) = \sum_{k=0}^n mv(k)(v(k-1) - v(k-2)) \quad (8)$$

where $E_{step}(k)$ is the energy calculated using the virtual inertia in a single step. We can then identify an analogy between (8) and (5). The area beneath the pressing/releasing path in the force vs. position schematic in Fig. 3 shows the input/output

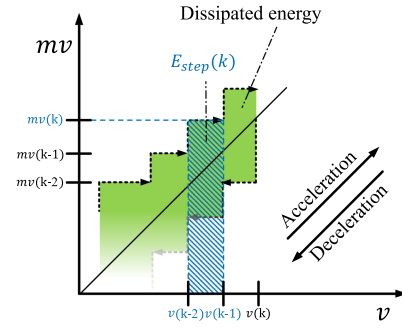


Fig. 4. Velocity versus momentum trajectory in a single contact. Signals are captured in between the haptic device and discrete interface.

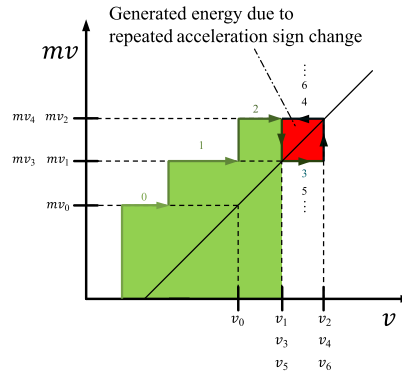


Fig. 5. Velocity versus momentum trajectory. Inertia might generate energy if the acceleration sign repetitively changes in every sample.

potential energy, which is expressed by (5). Similarly, the area beneath the acceleration/deceleration path in the momentum vs. velocity schematic in Fig. 4 shows the input/output kinetic energy, expressed by (8).

However, the major difference between Figs. 3 and 4 is that the virtual inertia dissipates energy, unlike the virtual spring. The vertical axis of Fig. 4 (mv) is not affected by delay; rather, the horizontal axis (v) is affected by the one-step delay ($k-1$). Note that the blue-shaded part ($E_{step}(k)$) in Fig. 4 has a delayed horizontal axis ($v(k-1) - v(k-2)$), which is related to its width. Therefore, in Fig. 4, a graph shift caused by the delay on the horizontal axis results in a clockwise hysteresis, whereas, in Fig. 3, a graph shift caused by the delay on the vertical axis results in a counterclockwise hysteresis.

As shown in Fig. 4, this causes the deceleration trajectory to remain lower than the acceleration trajectory and the interaction energy with virtual inertia to remain positive, as indicated by the green area in Fig. 4. Therefore, virtual inertia can be considered a passive element. This is an interesting conclusion because physical inertia is not an energy-dissipating element; rather, it is an energy storage element. However, when we use virtual (discrete) inertia, it has a certain energy dissipation capacity.

Although virtual inertia has the capacity to dissipate energy, it might generate energy when the acceleration sign repetitively changes in one sample time in certain scenarios (Fig. 5). The numbers in Fig. 5 and the subscripts in the velocity correspond to each other. As shown in Fig. 4, the one-step delay does not affect the vertical axis, but affects the horizontal axis. If the

velocity maintains its increasing or decreasing tendency for at least three steps (e.g., from v_0 to v_2), this behavior may not cause any energy leak. However, if the tendency changes in three steps, i.e., the acceleration sign changes in every sample time, the energy begins to leak (as graphically shown with the red counter-clockwise hysteresis in Fig. 5).

Note that this active behavior of virtual inertia can occur at any instance during haptic interaction, irrespective of whether the velocity is positive or negative. Moreover, this activity occurs at the equilibrium point owing to the velocity jittering near zero, which causes energy generation. Although virtual inertia can dissipate energy, this undesired energy leak impedes the use of inertia as an energy dissipation element, particularly in high-stiffness stable haptic interfaces.

However, the use of an acceleration signal is not straightforward, particularly in high-frequency noisy scenarios. There are two possible methods for this. One uses a normal low-pass filtered acceleration value from the encoder. According to [14], rendering the virtual inertia using low-pass filtered acceleration has no effect on the passivity of the system and even expands the stable range of virtual inertia. However, it would be desirable to use a low-pass filter with a minimum phase lag, for example, as in [22]. The other method uses the measured acceleration value from an accelerometer, which is more accurate than filtered values from the encoder because it directly measures the acceleration values rather than using mathematical operators such as integration or differentiation. However, certain filtering methods may be used because of the noise of the sensor itself. This type of filtering is acceptable in the same manner. Based on the encoder resolution of the haptic system, we may select a proper one between the filtered acceleration from the encoder or the measured acceleration from the accelerometer.

IV. UNIDIRECTIONAL VIRTUAL INERTIA

To overcome the limitation of conventional virtual inertia and enable the virtual inertia to properly dissipate the generated energy (even during high-frequency chattering scenarios), we propose the concept of unidirectionality to virtual inertia, similar to the concept of unidirectional damping [23], [24]. Here, the virtual inertia is only activated when the energy is stored. Although conventional virtual inertia (bidirectional inertia) has an energy dissipation ability, it is essentially an energy storage element. Depending on the sign of velocity and acceleration, the energy is stored or released, as shown in (7). However, using the unidirectional condition by vanishing the inertia after absorbing energy without returning it to the system, the unidirectional virtual inertia can be used as a pure energy dissipation element; moreover, the amount of dissipated energy can be significantly larger than that of the conventional one.

The following is the scheme of the proposed unidirectional virtual inertia:

$$m_{vir}(k) = \begin{cases} m, & \text{if } v(k)a(k-1) \geq 0, \\ 0, & \text{else.} \end{cases} \quad (9)$$

Inertia is only activated when the magnitude of velocity increases in either the positive or negative direction, which physically

Algorithm 1: Unidirectional Virtual Inertia.

```

for  $k = 1, 2, \dots, n$  do
   $f(k) = k_{vir}x(k)$  where  $k_{vir}$  is the stiffness of the VW
  if  $v(k)a(k-1) \geq 0$  then
     $m_{vir} = m$ 
  else
     $m_{vir} = 0$ 
  end if
   $f(k) = f(k) + m_{vir}a(k)$ 
end for

```

indicates that the system operates toward increasing the kinetic energy. Algorithm 1 shows the pseudo code for the implementation of the unidirectional virtual inertia.

Note that we use $k-1$ step accelerations to calculate a k -step unidirectional virtual inertia after considering the ZOH effect. As explained in the introduction, Fig. 1 shows a schematic of the proposed unidirectional virtual inertia.

As shown in (9), the unidirectional virtual inertia is only activated during the pressing phase with positive acceleration, and during the releasing phase with negative acceleration. This indicates that the unidirectional virtual inertia stores the generated energy from the system while it is active; moreover, it disappears with the stored energy when it is deactivated.

V. SIMULATIONS AND EXPERIMENTAL VALIDATIONS

A. Simulation

Although most available haptic interfaces are multi-degree-of-freedom (DoF) to facilitate force feedback for complex VEs, the simulations performed in this study considered a 1-DoF system to avoid being influenced by nonlinearities and cross-coupling effects over translational and rotational DoFs. The dynamics of the simulated haptic device (HD), human operator (HO), and VE are expressed as follows:

$$f_d + f_h = m_d a_d + b_d v_d \quad (10)$$

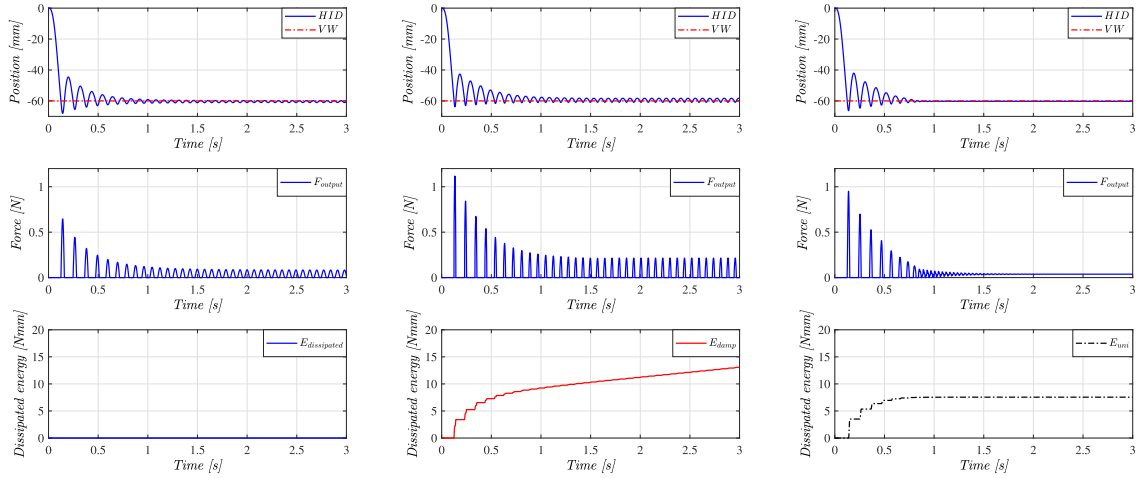
$$\tau_{op} - f_h = m_{op} a_d + b_{op} v_d + k_{op} x_d \quad (11)$$

$$f_d = -m_{vir} a_d - b_{vir} v_d - k_{vir} (x_d - x_{wall}) \quad (12)$$

where x_d , v_d , and a_d are the displacement, velocity, and acceleration of the HD, respectively; m_d and b_d are the mass and viscous coefficients of the HD, respectively; f_h is the force that the HO applies to the HD; f_d is the actuator-driving force of the HD, which is produced by the dynamics of the VE; m_{vir} , b_{vir} , and k_{vir} are the virtual mass, damping, and stiffness of the VE, respectively, and x_{wall} is the position of the VE. m_{op} , b_{op} , and k_{op} are the mass, viscous coefficient, and stiffness of the HO, respectively, while τ_{op} is the force generated by the muscles of the HO. The HO firmly grasps the HD and never releases it during the operation. The parameters of the HD and HO used for this simulation were as follows:

$$m_d = 0.01 \text{ kg}, b_d = 0.1 \text{ Ns/m.}$$

$$m_{op} = 0.01 \text{ kg}, b_{op} = 0.01 \text{ Ns/m}, k_{op} = 10 \text{ N/m.}$$



(a) With VW stiffness $k_{vir} = 0.08$ N/mm (b) With VW stiffness $k_{vir} = 0.15$ N/mm (c) With VW stiffness $k_{vir} = 0.15$ N/mm and no energy dissipative elements. and damping $b_{vir} = 0.0008$ Ns/mm. and unidirectional inertia $m_{vir} = 0.01$ kg.

Fig. 6. (a) With VW stiffness $k_{vir} = 0.08$ N/mm and no energy dissipative elements. (b) With VW stiffness $k_{vir} = 0.15$ N/mm and damping $b_{vir} = 0.0008$ Ns/mm. (c) With VW stiffness $k_{vir} = 0.15$ N/mm and unidirectional inertia $m_{vir} = 0.01$ kg. Simulation results with various dissipative elements.

Note that the HD and HO were simulated in the continuous time domain, whereas the virtual wall (VW) was simulated in the discrete domain at a sampling frequency of 1 kHz. Moreover, for the given HD and HO models with significantly low damping, the stiffness of the VW used in these simulations (0.15 N/mm) was already sufficiently high to make the interaction unstable. The acceleration of the HD was computed using the one-step backward discrete derivative of its velocity, which was also computed in a similar manner. To add the effects of real scenario to the simulation, a simulated sensor noise, (a band-limit white noise along with a low-pass filter), was added to the position signal of the HD. In addition, a quantization block in Simulink that discretizes the position signal of the HD and a 2 ms round-trip computational delay were added.

As explained in Section III, a unidirectional virtual inertia can eliminate high-frequency noise, which might not be possible with virtual damping. To validate this, we simulated a scenario where the HO penetrated slightly into a soft VW. The VW was located at -60 mm. The simulations results were as follows:

- 1) *Only $k_{vir} = 0.08$ N/mm:* Fig. 6(a) shows that owing to the absence of VW damping (b_{vir}), there were high-frequency limit cycles. Even without any VW damping, the contact did not become completely unstable because the damping of the HO and HD dissipated the energy generated by the discretization effect. Although the amplitude of the limit cycles was small, it might have cued undesired feedback to the HO; therefore, it was not preferred.
- 2) *$k_{vir} = 0.15$ N/mm, $b_{vir} = 0.0008$ Ns/mm:* The stiffness of VW increased to 0.15 N/mm to make the haptic interaction unstable. The VW damping value was then tuned to 0.0008 Ns/mm to stabilize the system. Fig. 6(b) shows that, although the haptic interaction did not diverge, the amplitude of the limit cycles was significantly large; it pushed the HO out of the wall. This was the best-tuned damping value, and any change resulted in the behavior becoming worse.

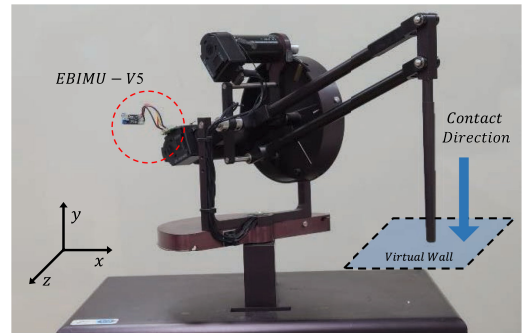


Fig. 7. PHANToM premium 1.5 for experimental evaluation. Only the Y-axis was used and an EBIMU-V5 IMU sensor was installed at the motor to measure the Y-axis acceleration.

- 3) *$k_{vir} = 0.15$ N/mm, $m_{vir} = 0.01$ kg:* Subsequently, the damping was replaced with a unidirectional virtual inertia of 0.01 kg. The addition of the unidirectional virtual inertia rather than damping stabilized the interaction and considerably reduced the amplitude of the high-frequency oscillations [see Fig. 6(c)]. The energy plot shows that the unidirectional virtual inertia was a passive element and aided in dissipating excess energy to stabilize the system.

B. Experiment

1) *Experimental Setup:* As Fig. 7 shows, a PHANToM Premium 1.5, which is extensively used in the haptic domain, was adopted for the experiments. The controller for the system was operated with a sampling rate of 1 kHz, and the VE comprised a VW modeled as a spring. The velocity obtained from the position encoder of the motors was used as the damping element. However, owing to the noisy behavior of the double derivative, acceleration was obtained from an inertial measurement unit (IMU) sensor for better accuracy. The IMU sensor, EBIMU-V5, was attached to the motor side, as indicated by the red dotted

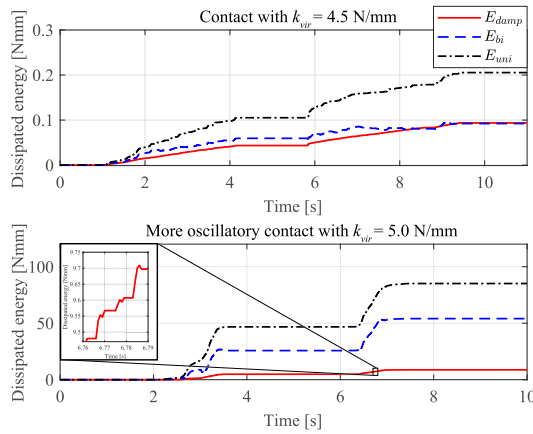


Fig. 8. Various energy dissipation ability of various elements. The dissipated energy from the virtual damping is the experimental result, and the dissipated energies from the two different types of virtual inertia are the simulated results using the virtual damping experiment.

circle in Fig. 7. The parameters for these experiments were best tuned to render the stiffnesses used. During the experiment, a human subject was asked to collide with a rendered flat virtual surface.

2) *Energy Dissipation and Contact Tasks*: Fig. 8 shows the energy behavior of three different dissipative elements in two scenarios. One was for a more oscillatory contact with a higher stiffness VW and the other for a less oscillatory contact with a lower stiffness VW. For a fair comparison, the energy response for a bi- and unidirectional virtual inertia of 0.0018 kg is shown based on the velocity and acceleration information obtained from experimental data for each higher/lower stiffness scenario. For a lower stiffness contact, a stiffness of 4.5 N/mm and a damping of 0.0027 Ns/mm were used. For the higher stiffness contact, the stiffness was increased to 5.0 N/mm, whereas the other conditions were the same as those in the stable scenario.

In both scenarios, these were hypothetical results; however, the energy behavior associated with both virtual inertias still dissipated more energy than the damping element. The vertical energy oscillations due to bidirectional virtual inertia confirmed the storage and release of energy, as described in Section III. Moreover, in the presence of a high-frequency velocity jitter, the energy did not accumulate monotonically at higher stiffness. This meant that the virtual damping not only dissipated energy but also generated it, particularly at high-frequency oscillations, reducing the ability of the damping to dissipate energy. This can be observed in the magnified subplot in Fig. 8; however, the unidirectional virtual inertia could effectively dissipate larger amounts of energy because it was a pure energy dissipation element.

Fig. 9(a) shows the limited performance of virtual damping. The force graph shows an unstable force feedback, F_{origin} is the original force feedback from the spring modeled VW, F_{output} is the controlled output force, F_{damp} is the force generated by the dissipative element, and k_{dis} is the displayed stiffness, which is computed by dividing the controlled output force by the penetration depth, $F_{output}/(x_d - x_{wall})$. Generally, virtual damping

has a certain limitation, as discussed in the introduction. Owing to this limitation, virtual damping cannot stabilize the haptic interaction with a VW of stiffness larger than 5.0 N/mm.

However, with the unidirectional virtual inertia, it is possible to stabilize the interaction without any stability issue as shown in Fig. 9(b). Because unidirectional virtual inertia can be easily removed under simple conditions when it is about to release energy, it can render a significantly higher stiffness in a stable manner than conventional virtual damping or bidirectional virtual inertia. This enabled a stable high-stiffness haptic interaction, where the mean of the displayed stiffness was 5.4968 N/mm, which was very close to the desired stiffness of 5.5 N/mm for two consecutive contacts, which was not possible using only the virtual damping, as shown in Fig. 9(b).

3) *Stable Range for Each Dissipative Element*: For each dissipative element (damping, bi- and unidirectional virtual inertia), we experimentally investigated the parameter ranges that can be applied without stability issue; these are plotted in Fig. 10. For a given stiffness of the VW from 2.5 N/mm with 0.5 N/mm upward regular intervals, we applied and swept each single energy dissipation element and observed a stable interaction region with no unwanted vibration. During the investigation of the single energy dissipation element, the other elements were set to zero.

For low-stiffness VW, a wide range of virtual damping could be injected without ruining stability; however, the range of applicable virtual damping rapidly decreased with an increase in stiffness. When the stiffness value reached 4.5 N/mm, no value of virtual damping could be injected without stability issue. The bidirectional virtual inertia's maximum renderable stiffness was also 4.5 N/mm, similar to virtual damping; in contrast, the unidirectional virtual inertia had a significantly larger and wider stable region. We expected the unidirectional virtual inertia overlap with the bidirectional inertia region because the unidirectional virtual inertia must dissipate more energy with the same value of inertia. However, interestingly, in our experimental results, the two different types of virtual inertias had exclusive regions, particularly for lower values of inertia. We plan to further investigate this in future research.

4) *Stable Range for Combined Dissipative Elements*: Furthermore, we experimentally verified the effect of simultaneously using two dissipative elements, i.e., virtual damping and unidirectional virtual inertia. We assumed that virtual damping and unidirectional virtual inertia would dissipate the different types of generated energy owing to the different operating phases. Fig. 11 shows the stable interaction range when both virtual damping and unidirectional virtual inertia were simultaneously applied.

The stiffness of the VW was rendered similarly, as shown in Fig. 10. However, in this experiment, the virtual damping was swept while the unidirectional virtual inertia was fixed. The stable boundary points of the experiment with the unidirectional virtual inertia were used to render the 0.5 N/mm increased stiffness of the VW, which was unstable without virtual damping. Here, we swept the virtual damping at 0.0001 Ns/mm interval, in order to find a stable interaction region with no unwanted vibration. Note that the nonlinearity observed in the figure can

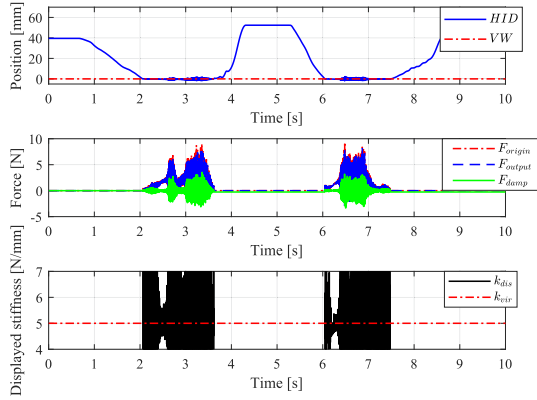
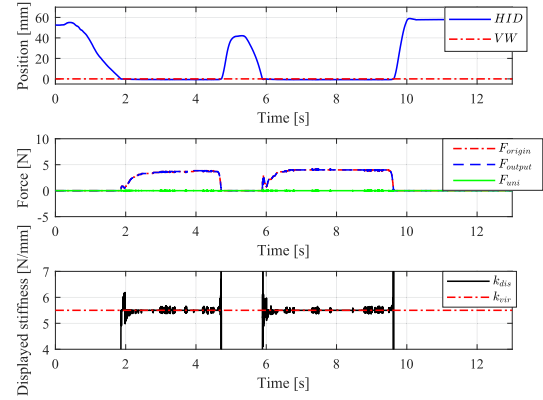
(a) With only virtual damping for $k_{vir}=5.0$ N/mm VW stiffness(b) With only unidirectional virtual inertia for $k_{vir}=5.5$ N/mm VW stiffness

Fig. 9. (a) With only virtual damping for $k_{vir}=5.0$ N/mm VW stiffness. (b) With only unidirectional virtual inertia for $k_{vir}=5.5$ N/mm VW stiffness. Comparison of experimental results between virtual damping only and the unidirectional virtual inertia only.

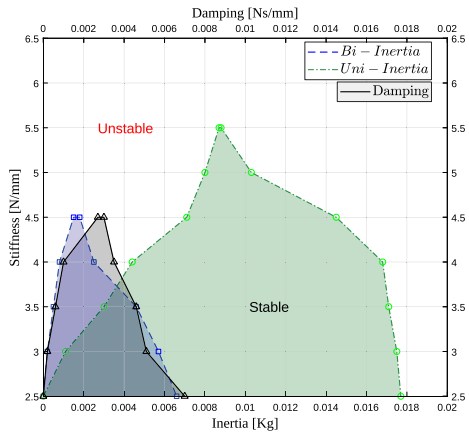


Fig. 10. Stable range of various dissipative elements.

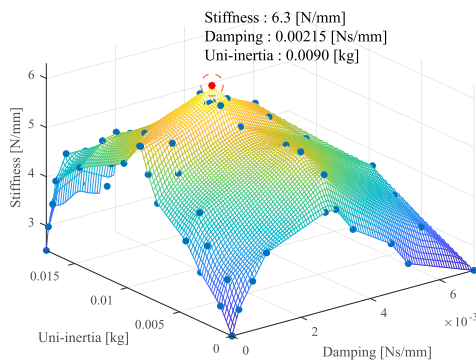


Fig. 11. 3D stable region when both virtual damping and unidirectional virtual inertia are implemented.

be explained by the human factor, as well as the limited number of experimental data for averaging out. Although the mesh plot was nonlinear, it was sufficiently clear to show this tendency. The maximum stiffness that could be rendered using our setup was 6.3 N/mm, where the values of virtual damping and unidirectional virtual inertia were 0.00215 Ns/mm and 0.0090 kg,

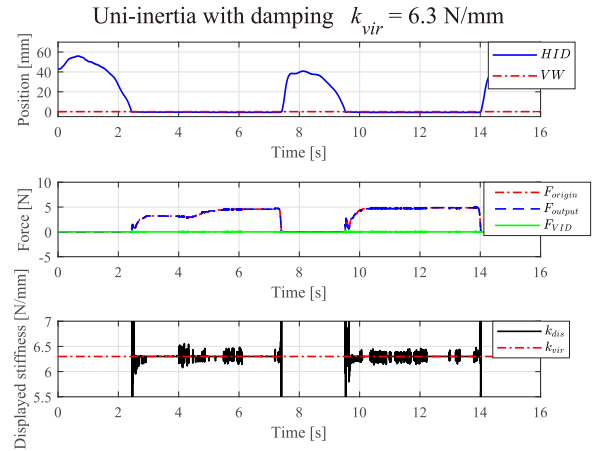


Fig. 12. Unidirectional virtual inertia with damping can render significantly higher stiffness compared with other scenarios.

respectively. Fig. 12 shows the results of using virtual damping with unidirectional virtual inertia as the inferred parameters. Each energy dissipative element was optimized to render haptic interaction with high stiffness. We confirmed that the mean of the displayed stiffness was 6.2987 N/mm, which was almost equal to the desired stiffness of the VW of 6.3 N/mm during contact. The rate of increase of the displayed stiffness during high-stiffness wall contact was also instantaneous, which was perceived by the HO as a hard contact.

Fig. 13 shows the contribution of each energy dissipative element with a stiffness of 6.3 N/mm. The unidirectional virtual inertia could dissipate a larger amount of energy than virtual damping over the entire interaction; meanwhile, the energy dissipation of the virtual damping was concentrated at the start and end of the contact. This can be explained by the sufficiently large acceleration contribution, even during the extreme low-velocity interaction in the middle of the contact. These two different energy dissipative patterns can be used in a complementary manner.

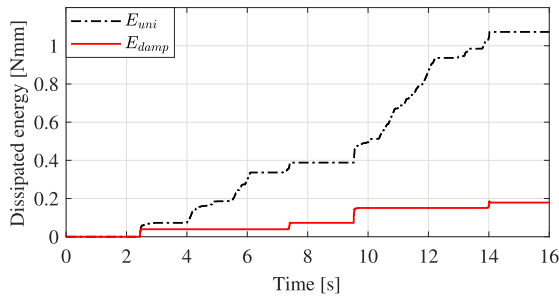


Fig. 13. Energy contributions of two different types of energy dissipative elements.

VI. CONCLUSION AND FUTURE RESEARCH

This paper investigates the possibility of using virtual inertia as an energy dissipation element for stable haptic interfaces. We observed that virtual inertia can dissipate energy even during high-velocity interactions, unlike virtual damping. Furthermore, we propose a unidirectional virtual inertia, for the first time, to dissipate a considerable amount of energy compared with conventional virtual inertia and virtual damping. By storing energy to the virtual inertia in the kinetic energy-increasing phase and making it disappear before returning the energy to the system in the kinetic energy-decreasing phase, we realized unidirectional virtual inertia as an energy dissipation element. The feasibility and performance of the proposed method were verified using simulations and PHANTOM-based experiments. Both studies verified the outstanding amount of energy dissipation capacity of unidirectional virtual inertia; moreover, we observed that applying two dissipative elements (virtual damping and unidirectional virtual inertia) simultaneously would increase the energy dissipation capacity even further, and therefore enable a larger stiffness interaction without a stability issue.

It is assumed that virtual damping and unidirectional virtual inertia can exclusively dissipate the energy produced because of their different operating conditions. Virtual damping dissipates the produced energy during the lower velocity interaction; however, the unidirectional virtual inertia can dissipate the produced energy during the higher velocity interaction. Therefore, we expect that using both dissipative elements simultaneously increases the stable impedance range. However, further investigation is required to prove this mathematically and experimentally. When we determine a method of calculating the necessary amount of unidirectional virtual inertia for the corresponding energy dissipation, we will develop a new time-domain passivity approach using the adaptive unidirectional virtual inertia along with the adaptive virtual damping in a complementary manner, such as using virtual inertia in a scenario in which the virtual damping cannot properly dissipate energy. The proposed unidirectional virtual inertia may create a new horizon for any controller that requires energy dissipation elements.

REFERENCES

- [1] J. E. Colgate and G. G. Schenkel, "Passivity of a class of sampled-data systems: Application to haptic interfaces," *J. Robot. Syst.*, vol. 14, no. 1, pp. 37–47, 1997.
- [2] J. J. Abbott and A. M. Okamura, "Effects of position quantization and sampling rate on virtual-wall passivity," *Trans. Robot.*, vol. 21, no. 5, pp. 952–964, 2005.
- [3] T. H. Do and J.-H. Ryu, "Memory based passivation method for stable haptic interaction," in *Proc. IEEE World Haptics Conf.*, 2011, pp. 409–414.
- [4] R. J. Adams and B. Hannaford, "Stable haptic interaction with virtual environments," *Trans. Robot. Autom.*, vol. 15, no. 3, pp. 465–474, 1999.
- [5] J. E. Colgate, M. C. Stanley, and J. M. Brown, "Issues in the haptic display of tool use," in *Proc. Int. Conf. Intell. Robot. Syst.*, vol. 3, 1995, pp. 140–145.
- [6] J.-P. Kim and J. Ryu, "Energy bounding algorithm based on passivity theorem for stable haptic interaction control," in *Proc. 12 Symp. Haptic Interfaces Virtual Environ. Teleoperator Syst.*, 2004, pp. 351–357.
- [7] B. Hannaford and J.-H. Ryu, "Time-domain passivity control of haptic interfaces," *Trans. Robot. Autom.*, vol. 18, no. 1, pp. 1–10, 2002.
- [8] H. Singh, D. Janetzko, A. Jafari, B. Weber, C. I. Lee, and J.-H. Ryu, "Enhancing the rate-hardness of haptic interaction: Successive force augmentation approach," *IEEE Trans. Ind. Electron.*, vol. 67, no. 1, pp. 809–819, Jan. 2020.
- [9] A. Jafari, M. Nabeel, and J. H. Ryu, "The input-to-state stable (ISS) approach for stabilizing haptic interaction with virtual environments," *IEEE Trans. Robot.*, vol. 33, pp. 948–963, Aug. 2017.
- [10] T. Hulin, R. G. Camarero, and A. Albu-Schäffer, "Optimal control for haptic rendering: Fast energy dissipation and minimum overshoot," in *Proc. Int. Conf. Intell. Robot. Syst.*, 2013, pp. 4505–4511.
- [11] N. Colonnesse and A. M. Okamura, "M-width: Stability and accuracy of haptic rendering of virtual mass," in *Proc. Really Simple Syndication*, 2012, pp. 9–13.
- [12] J. J. Gil, A. Ugartemendia, and I. Diaz, "Stability analysis and user perception of haptic rendering combining virtual elastic, viscous and inertial effects," *Appl. Sci.*, vol. 10, no. 24, p. 8807, 2020.
- [13] I. Desai, A. Gupta, and D. Chakraborty, "Virtual mass feedback for rendering stiff virtual springs," in *Proc. IEEE World Haptics Conf.*, 2019, pp. 211–216.
- [14] N. Colonnesse and A. M. Okamura, "M-width: Stability, noise characterization, and accuracy of rendering virtual mass," *Int. J. Rob. Res.*, vol. 34, no. 6, pp. 781–798, 2015.
- [15] M. Mahvash and A. M. Okamura, "Enhancing transparency of a position-exchange teleoperator," in *Proc. IEEE World Haptics Conf.*, 2007, pp. 470–475.
- [16] G. Aguirre-Ollinger, J. E. Colgate, M. A. Peshkin, and A. Goswami, "Design of an active one-degree-of-freedom lower-limb exoskeleton with inertia compensation," *Int. J. Rob. Res.*, vol. 30, no. 4, pp. 486–499, 2011.
- [17] J. J. Gil, A. Rubio, and J. Savall, "Decreasing the apparent inertia of an impedance haptic device by using force feedforward," *IEEE Trans. Control. Syst. Technol.*, vol. 17, no. 4, pp. 833–838, Jul. 2009.
- [18] S. Fahmi and T. Hulin, "Inertial properties in haptic devices: Non-linear inertia shaping vs. force feedforward," *IFAC-PapersOnLine*, vol. 51, no. 22, pp. 79–84, 2018.
- [19] J. C. Willems, "Dissipative dynamical systems Part I: General theory," *Arch. Ration. Mech. Anal.*, vol. 45, no. 5, pp. 321–351, 1972.
- [20] A. J. Van Der Schaft and A. Van Der Schaft, *L2-Gain and Passivity Techniques in Nonlinear Control*, vol. 2. Berlin, Germany: Springer, 2000.
- [21] J.-H. Ryu, Y. S. Kim, and B. Hannaford, "Sampled- and continuous-time passivity and stability of virtual environments," *IEEE Trans. Robot.*, vol. 20, no. 4, pp. 772–776, Aug. 2004.
- [22] F. Janabi-Sharifi, V. Hayward, and C.-S. Chen, "Discrete-time adaptive windowing for velocity estimation," *IEEE Trans. Control Syst. Technol.*, vol. 8, no. 6, pp. 1003–1009, Nov. 2000.
- [23] M. Sakaguchi, J. Furusho, and N. Takesue, "Passive force display using ER brakes and its control experiments," in *Proc. Virtual. Real.*, 2001, pp. 7–12.
- [24] L. B. Rosenberg and B. D. Adelstein, "Perceptual decomposition of virtual haptic surfaces," in *Proc. Radial Flux Variable Reluctance Resolvers*, 1993, pp. 46–53.